

## 6 EOT analysis of Queensland rainfall in HiGEM

In this section, the leading four EOTs of HiGEM seasonal Queensland rainfall are introduced (Section 5.1) then compared to the leading three EOTs of SILO seasonal rainfall, as discussed in Section 2.7. Appendix A reproduces the spatial patterns (Fig. 24) and time series (Fig. 25) of the SILO EOTs, as well as the tables giving the correlations with proposed large-scale modes (Table 3) and the mechanisms that Klingaman (2012b) concluded drove each EOT (Table 4).

### 6.1 Spatial and temporal patterns

As for the SILO EOTs in Klingaman (2012b), the leading seasonal HiGEM EOTs display a uni-polar spatial pattern, indicating that they describe coherent variations in rainfall across much of Queensland (Figs. 11a–d). EOT 1 for DJF (Fig. 11a) and MAM (Fig. 11b) are concentrated in the north, as in SILO (Figs. 24a and 24b). The central point in the HiGEM MAM EOT 1, however, is located much further north and west than in the corresponding SILO EOT, with lower correlations in south-eastern Queensland. JJA EOT 1 in HiGEM (Fig. 11c) is nearly identical to that from SILO (Fig. 24c), while SON EOT 1 (Fig. 11d) is shifted south relative to SILO (Fig. 24d) with weak correlations in north-eastern Queensland. These spatial shifts suggest a more abrupt seasonal transition in HiGEM between the summer rainfall regimes—when the rain is heaviest in the north of Queensland—and the winter regime—when the south of the state receives more rain than the north.

Once the leading EOTs have been removed, the remaining HiGEM EOTs describe coherent regional variations in seasonal rainfall. The spatial patterns of HiGEM EOTs 2–4 generally show less agreement with those from SILO. Even slight differences in the spatial patterns of the first EOTs can cause considerable changes in the remaining EOTs, since each EOT depends upon the ones preceding it. These differences become compounded in EOTs beyond the second, as EOT 3, for example, depends on the first two EOTs. Also, EOTs beyond the first explain similar percentages of the total variance in both HiGEM (Table 1) and SILO (Table 3). Small variations in these percentages between HiGEM and SILO, then, could lead to differences in the order of the EOTs, which again would affect the lower-order patterns as each EOT depends upon the ones preceding it. For these reasons, the first six EOTs from HiGEM were computed to compare with the three leading SILO EOTs, although none of the HiGEM EOTs 5 or 6 were similar to any of the SILO EOTs 1–3 (section 2.7). Still, there are some notable similarities between the regional HiGEM and SILO EOTs, including HiGEM DJF EOT 4 (Fig. 11i) and SILO DJF EOT 2 (Fig. 24e), HiGEM JJA EOTs 2 and 3 (Figs. 11g and 11k) and their SILO counterparts (Figs. 24g and 24k) and HiGEM SON EOT 4 (Fig. 11p) and SILO SON EOT 3 (Fig. 24l). The following sub-sections will evaluate whether the HiGEM EOTs are driven by the same mechanisms as those from SILO.

Time series of each HiGEM EOT are shown in Figure 12. As for the SILO EOTs (Fig. 25), there are practically no statistically significant 31-year running linear trends in the HiGEM EOTs, shown by the scarcity of red dots along the horizontal axes of Figure 12. While SILO DJF EOT 1 demonstrated considerable decadal and multi-decadal variability, which Klingaman (2012b) showed was associated with the IPO (see Fig. 5a in that report), the wavelet transform of HiGEM DJF EOT 1 displays only limited 8–10 year variability for a portion of the simulation (Fig. 13a). This is consistent with the lack of both decadal variability in Queensland rainfall (section 3) and an IPO (section 4.2) in HiGEM. Several other, regional HiGEM rainfall EOTs do show some decadal and multi-decadal variability, however, particularly JJA EOT 2 and SON EOT 4 (Figs. 13d and 13e, respectively); DJF EOT 2 and MAM EOT 2 also have limited power on these temporal scales (Figs. 13b and 13c, respectively). Of these, the spatial patterns of HiGEM DJF EOT 2, MAM EOT 2 and JJA EOT 2 resemble SILO DJF EOT 3, MAM EOT 2 and JJA EOT 2, respectively; these SILO EOTs also demonstrated decadal or multidecadal variability in Klingaman (2012b) (see Fig. 5 in that report) which was shown to be driven by internal variations in local synoptic circulation patterns (e.g. onshore winds). Section 5.2.4 analyses whether the corresponding HiGEM EOTs are driven by similar mechanisms. While the spatial pattern of HiGEM SON EOT 4 (Fig. 11p) is similar to SILO SON EOT 3 (Fig. 24l), the SILO EOT did not display any decadal or multi-decadal variability.

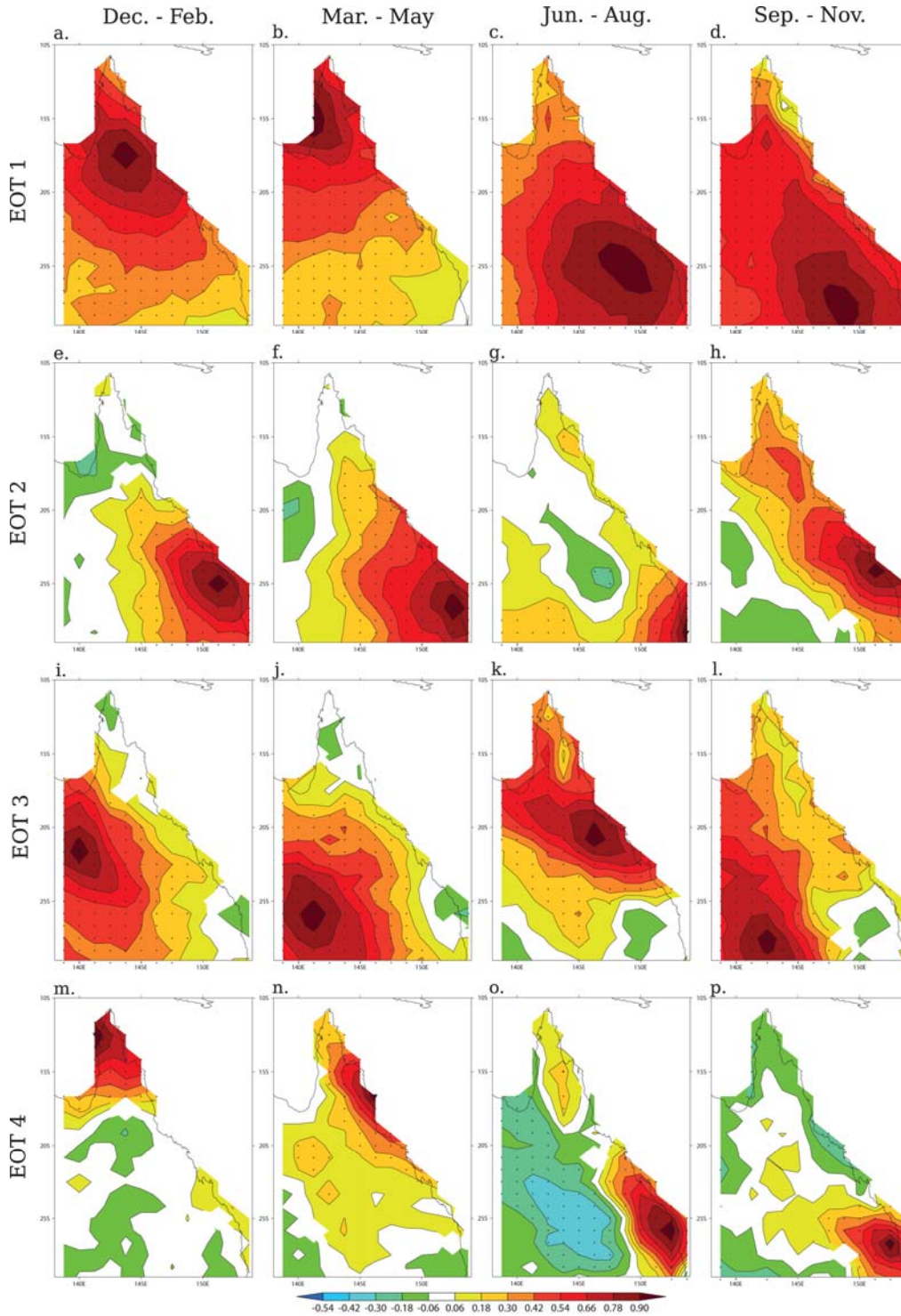


Figure 11: Spatial patterns of the first four empirical orthogonal teleconnections (EOTs) of seasonal HiGEM Queensland rainfall, using years 21–150 of the control integration, computed as the correlations of each grid point with the central grid point for each EOT (marked with a black triangle). Stippling indicates statistically significant correlations at the 5 per cent level.

## 6.2 HiGEM EOTs with SILO counterparts

In this section, those HiGEM EOTs with clear SILO counterparts—both in the region affected and in the mechanism producing rainfall variations—are analysed. As in Klingaman (2012b), the discussion of the EOTs is

divided by mechanism: the ENSO (Section 5.2.1), tropical cyclones (Section 5.2.2), the continental-scale monsoon circulation (Section 5.2.3) and local synoptic circulations (Section 5.2.4). Section 5.3 discusses those HiGEM EOTs 1–3 that do not match those from SILO. As four HiGEM EOTs are compared against only three from SILO, there will clearly be one additional, non-matching HiGEM EOT in each season. The non-matching HiGEM EOT in each season that explains the least variance is analysed briefly in Section 5.4 as an "additional EOT"; in MAM, JJA and SON this is EOT 4, while in DJF it is EOT 3. Table 2 shows, for each HiGEM EOT, the percentage of variance explained, the region affected, the driving mechanism and the matching SILO EOT, if any. A similar table for SILO can be found in Appendix A as Table 4.

The relevant regressions (e.g. on SSTs, 850 hPa winds, mean-sea-level pressure) from HiGEM on each EOT will be shown alongside those from observations and reanalysis. The latter regressions are reproduced from Klingaman (2012) for convenience; the data sources are not repeated here, however. For consistency, the figure captions refer to all regressions onto EOTs computed from SILO rainfall analyses as "SILO EOTs", instead of using the name of the observed dataset or reanalysis (e.g. HadISST for SSTs, the 20th Century Reanalysis (20CR) for atmospheric circulation fields).

### 6.2.1 ENSO-driven patterns

The leading, state-wide HiGEM rainfall EOTs in DJF, JJA and SON show statistically significant correlations with Niño 4 (Table 1), as for SILO (Table 3). HiGEM produces equatorial Pacific SST anomalies in association with DJF EOT 1 that resemble ENSO (Fig. 14a), but these are meridionally confined and extend too far west compared to the regression of HadISST SSTs on SILO DJF EOT 1 (Fig. 14d). HiGEM also lacks the extra-tropical Pacific SST anomalies in each hemisphere found in HadISST, which Klingaman (2012b) determined were the signature of the IPO; SILO DJF EOT 1 is strongly correlated with the IPO (Table 3). This further suggests the lack of an IPO in HiGEM. The DJF EOT 1 low-level circulation pattern in HiGEM (Fig. 14g) broadly agrees with that from the 20CR for the SILO EOT (Fig. 14j), with an enhanced monsoon cyclone over continental Australia. The cyclone is shifted too far east in HiGEM, however, and there is no sign of the positive pole of the Southern Oscillation, which appears in 20CR. The region of anomalous equatorial convergence in HiGEM is centred over the Maritime Continent, further west than in 20CR, which is consistent with a westward displacement of the anomalous Walker Circulation in HiGEM due to the extension of the ENSO-driven SST anomalies into the West Pacific. The combination of the displacements to the anomalous Walker Circulation and monsoon anticyclone in HiGEM produces an erroneous anomalous anti-cyclonic circulation in the Coral Sea northeast of Australia.

The HiGEM SST patterns associated with JJA EOT 1 (Fig. 14b) and SON EOT 1 (Fig. 14c) are in closer agreement with observations (Figs. 14e and 14f, respectively) than those for DJF EOT 1. In each season, though, the maximum HiGEM SST variability occurs in the central Pacific—close to the Niño 4 region—whereas the HadISST observations show equal amounts of variability in the central and eastern Pacific.

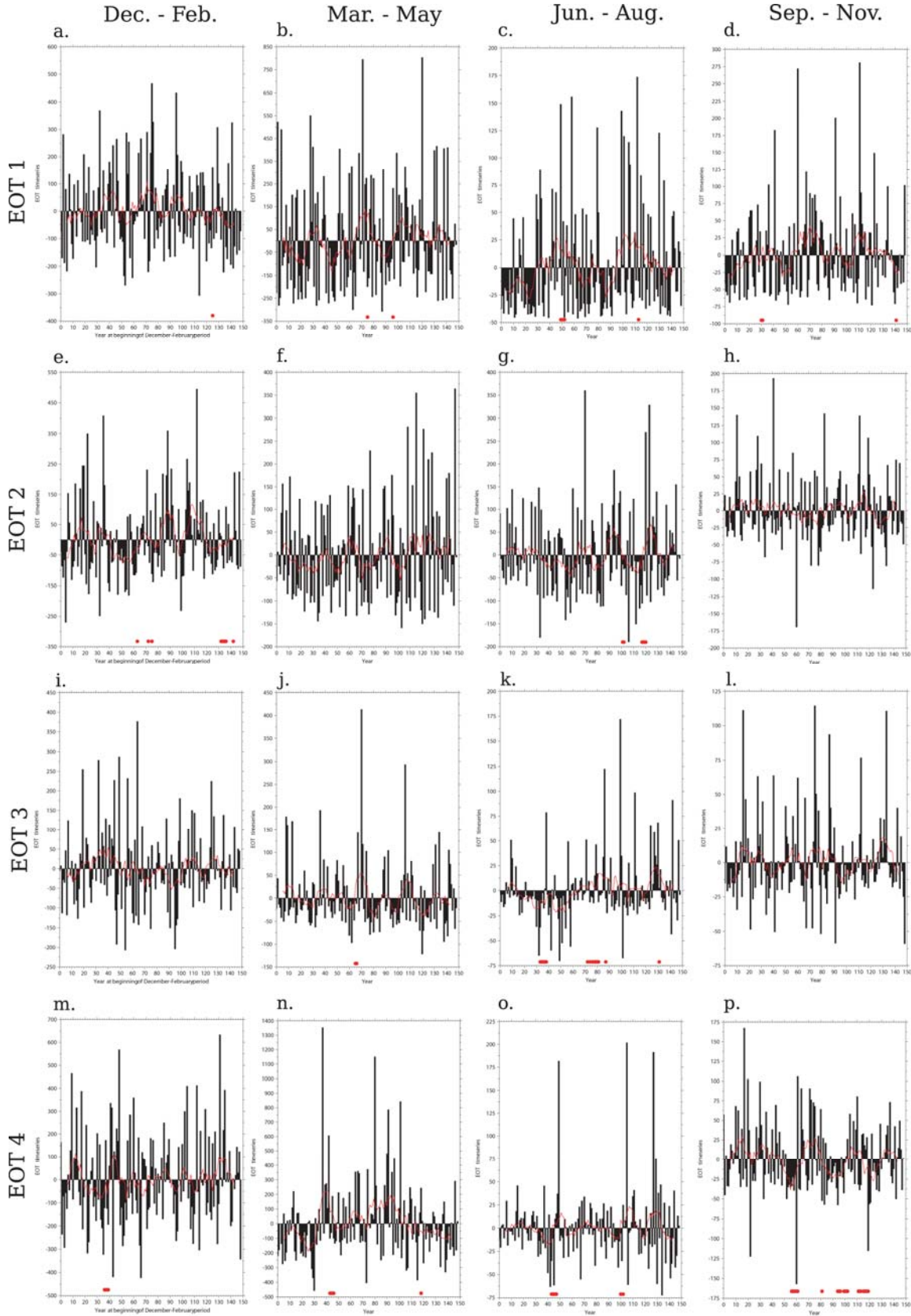


Figure 12: Time series of each of the four leading EOTs of seasonal HiGEM Queensland rainfall, arranged as for the spatial patterns in Fig. 11. The time series are expressed as anomalies from their mean, to aid interpretation. Red dots along the horizontal axis indicate where the 31-year running linear trend, computed using the 15 years before and after the dot, is statistically significant at the 5 per cent level.

Season and EOT	Variance explained	Niño 4	B <sub>120–150</sub>	B <sub>150–180</sub>	SAM	SAM <sub>Niño 4</sub>	IOD	IOD <sub>Niño 4</sub>
<b>December–February</b>								
EOT 1	32.18%	-0.28**	0.21*	0.23*	0.10	0.09	-0.16*	-0.08
EOT 2	9.80%	-0.15	0.27**	0.18*	0.16	0.14	-0.10	0.01
EOT 3	7.86%	-0.03	-0.08	-0.03	-0.05	-0.05	-0.05	-0.04
EOT 4	7.10%	-0.02	-0.06	-0.04	0.06	0.06	0.04	0.06
<b>March–May</b>								
EOT 1	28.59%	-0.10	-0.21*	-0.10	0.08	0.08	0.06	0.06
EOT 2	14.55%	-0.14	0.24**	0.13	0.16	0.15	0.08	0.08
EOT 3	7.10%	-0.25*	0.20*	0.03	0.11	0.10	-0.01	-0.01
EOT 4	7.00%	-0.14	0.01	-0.05	0.02	0.01	0.09	0.09
<b>June–August</b>								
EOT 1	46.56%	-0.37**	0.23*	-0.00	0.11	0.07	-0.27**	-0.15
EOT 2	16.39%	0.04	0.29**	0.25**	0.27**	0.28**	0.14	0.14
EOT 3	6.90%	-0.09	-0.11	-0.09	0.07	0.06	-0.25**	-0.23**
EOT 4	4.23%	-0.05	-0.00	-0.09	0.00	-0.00	0.13	0.16
<b>September–November</b>								
EOT 1	48.60%	-0.53**	0.40**	0.17	0.42**	0.36**	-0.38**	-0.10
EOT 2	9.89%	-0.15	0.11	0.21*	0.15	0.12	-0.13	-0.05
EOT 3	7.75%	-0.24**	0.09	0.26**	0.08	0.13	-0.18*	-0.05
EOT 4	4.00%	-0.07	-0.07	-0.14	0.11	0.09	-0.05	-0.01

Table 1: For the leading four HiGEM EOTs of seasonal rainfall: the percentage of variance in the area-averaged Queensland rainfall that the EOT explains; instantaneous correlation coefficients between each EOT and Niño 4 SSTs, the Bureau of Meteorology blocking index longitude averaged over 120°–150°E (B120–150) and 150°E–180° (B150–180), the Marshall (2003) index of the Southern Annular Mode (SAM) and the Saji et al. (1999) index of the Indian Ocean Dipole (IOD). For the SAM and the IOD, the partial correlations with Niño 4 SSTs are also computed (SAM<sub>Niño 4</sub> and IOD<sub>Niño 4</sub>, respectively). A \* (\*\*) indicates the correlation is statistically significant at the 5 per cent (1 per cent) level.

HiGEM correctly generates warm SST anomalies near Australia and the Maritime Continent during high JJA and SON EOT 1 years, consistent with La Niña in the central Pacific. There are strong suggestions of negative IOD events during wet springs in both HiGEM and observations, although the correlation with the IOD is statistically significant only in HiGEM (compare SON EOT 1 in Tables 1 and 3). Neither HiGEM nor HadISST produce a statistically significant partial correlation between the IOD and SON EOT 1, however, once the effects of Niño 4 have been removed from each. This suggests that the IOD and ENSO co-vary in HiGEM and in observations; past studies have concluded that the IOD does not influence eastern Australian rainfall independently from ENSO (e.g. Nicholls 1989; Murphy and Ribbe 2004; Risbey et al. 2009).

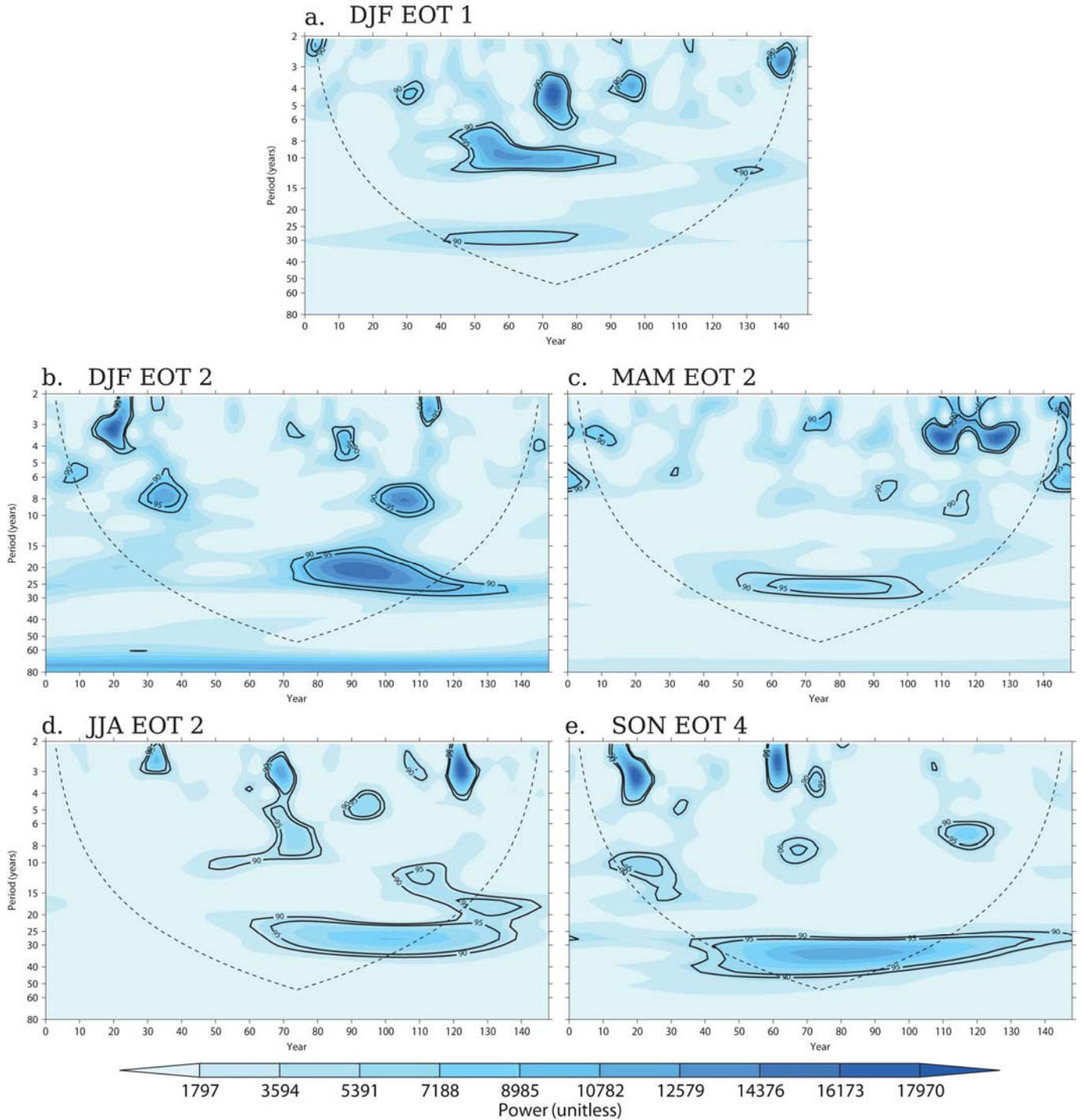


Figure 13: Wavelet transforms of selected HiGEM EOTs, using a Morlet mother wavelet. The 90 per cent and 95 per cent confidence intervals are drawn in thick solid contours and labelled. The dashed contour represents the cone of influence, outside of which the edge effects of the wavelet filtering technique dominate and the results cannot be trusted.

State-wide Queensland rainfall in winter and spring is associated with tropical and extra-tropical lower tropospheric circulation anomalies in HiGEM (Figs. 14h and 14i), as in 20CR (Figs. 14k and 14l). Klingaman (2012b) hypothesised that the extra-tropical circulation anomalies, which in observations were correlated with the SAM, could be explained only as the combined effects of the ENSO and the SAM as the partial correlations between the SAM and the EOT 1 patterns, removing the influence of Niño 4 on both, was statistically significant (Table 3). HiGEM produces a strong correlation with the SAM in spring (Table 1), which in observations remains significant when the partial correlation with Niño 4 is computed, but there is no significant correlation in winter. State-wide

JJA rainfall in HiGEM is therefore related to only the ENSO-driven tropical circulation. The relationships between these EOTs and the SAM will be examined further in Section 5.2.5. The 850 hPa circulations over Queensland in HiGEM (Figs. 14h–i) are remarkably similar to those from 20CR (Figs. 14j–k), with enhanced cyclonic circulation over northern Australia and anomalous onshore winds along the Queensland coast in both winter and spring. The strong blocking anti-cyclone over New Zealand during wet SON seasons in Queensland is also reproduced well in HiGEM.

Season and EOT	Variance explained	Region affected	Likely driving mechanism	Matching SILO EOT
December–February				
EOT 1	32.18%	State-wide	ENSO (peaking) effects on Australian monsoon	DJF EOT 1
EOT 2	9.80%	Southern	Coastal cyclonic activity and moisture transport	DJF EOT 3
EOT 3	7.86%	Northwestern	Enhanced local monsoon circulation and moisture transport	None
EOT 4	7.10%	Cape York	Tropical cyclone activity in the Coral Sea	DJF EOT 2
March–May				
EOT 1	28.59%	State-wide	Late-season monsoon circulation, but weaker than observed	MAM EOT 1
EOT 2	14.55%	Central and southern	Coastal cyclonic activity	MAM EOT 2
EOT 3	7.10%	Western	Weak ENSO (decaying) relationship	None
EOT 4	7.00%	Northern coastal	Tropical cyclone activity in the Coral Sea	None
June–August				
EOT 1	46.56%	State-wide	ENSO (developing) and onshore winds	JJA EOT 1
EOT 2	16.39%	Southeastern	Blocking in Southern Ocean and onshore winds	JJA EOT 2
EOT 3	6.90%	Northern	Southward moisture advection across Cape York	None
EOT 4	4.23%	Southeastern and western	Unknown, no significant regressions	None
September–November				
EOT 1	48.60%	State-wide	ENSO (developing), Southern Ocean blocking and the SAM	SON EOT 1
EOT 2	9.89%	Coastal and northern	Moist air and low pressures offshore	None
EOT 3	7.75%	Western	ENSO (decaying)	None
EOT 4	4.00%	Southeastern	Unknown, no significant regressions	None

Table 2: For each HiGEM EOT of seasonal rainfall, the percentage of variance in the all-Queensland rainfall that the EOT explains, the region of Queensland most affected by the EOT, the mechanism likely responsible for driving the EOT, and whether the EOT matches one of the leading three EOTs from SILO, both in terms of its spatial location and its driving mechanism.

Lag regressions of monthly-mean Niño 4 SSTs are used to evaluate whether HiGEM shows the same temporal evolution of Niño 4 SSTs associated with each ENSO-driven EOT as in observations (Fig. 15). For the leading summer and winter EOTs (Figs. 15a and 15c), HiGEM shows considerably lower regression coefficients than observations (Figs. 15b and 15d); HiGEM also lacks the observed peak in Niño 4 SST anomalies in DJF. Further examination reveals that this is due to a low standard deviation in Niño 4 SSTs in HiGEM, not to a low correlation coefficient (not shown). Regressions on HiGEM DJF EOT 1 show erroneous positive correlations in the following austral spring, which provides further evidence of the overly bi-annual ENSO variability in HiGEM identified in the lead–lag correlations of Niño 4 and Queensland rainfall (Fig. 6b). Only SON EOT 1 in HiGEM is related to strengthening Niño 4 SSTs that peak in the following DJF, as in HadISST.

There are two additional HiGEM EOTs—MAM EOT 3 and SON EOT 3—that show statistically significant correlations with Niño 4. While SILO also has one EOT in MAM (MAM EOT 3) and a second EOT in SON (SON EOT 2) that are driven by ENSO (Table 4), these HiGEM EOTs influence different regions of Queensland than the SILO EOTs: HiGEM MAM EOT 3 and SON EOT 3 describe rainfall variability in southwestern Queensland, while SILO MAM EOT 3 and SON EOT 2 are restricted to the tropical north. As these HiGEM EOTs do not agree with SILO, they are discussed in Section 5.3.1.

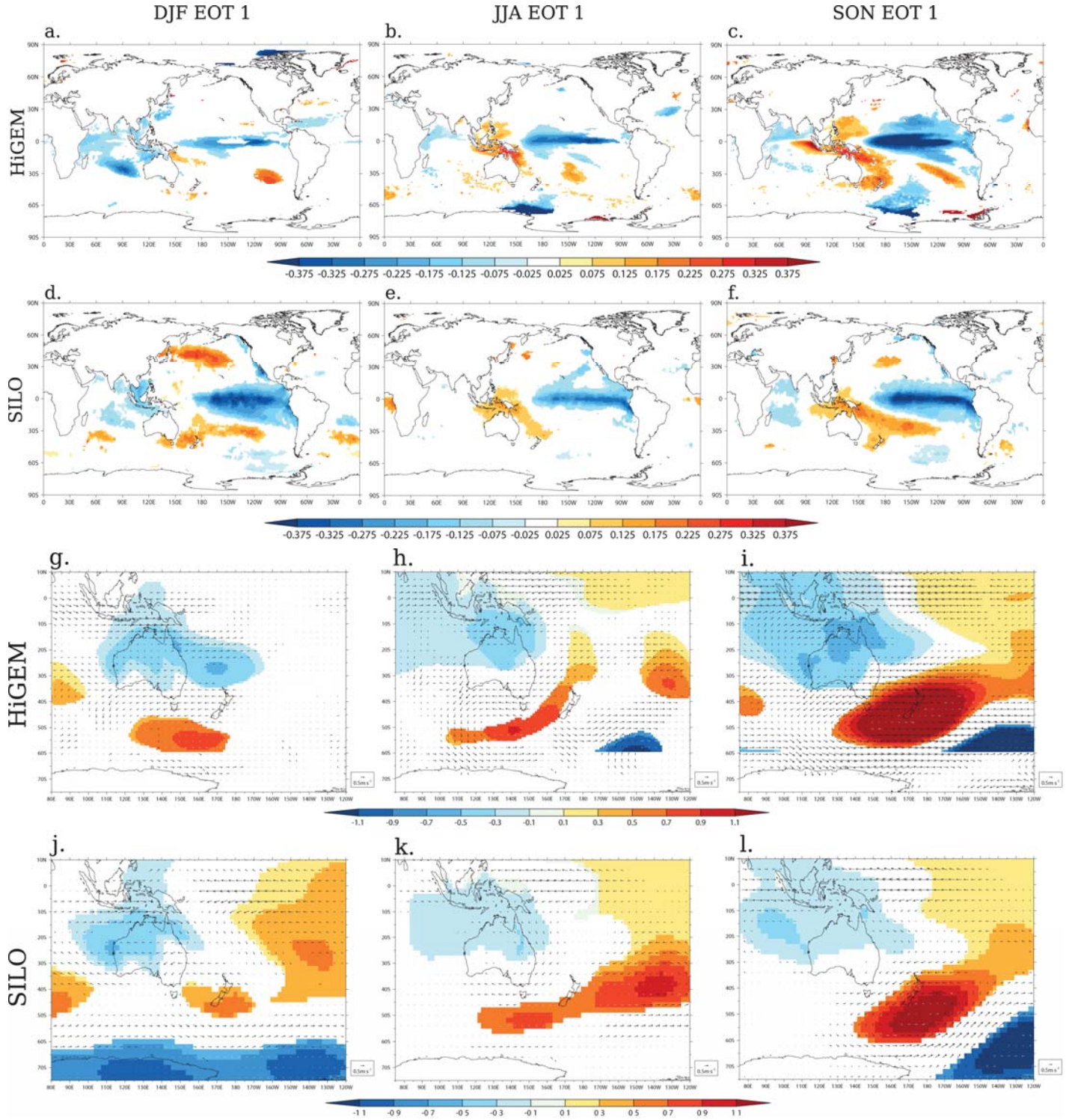


Figure 14: For the three HiGEM EOTs driven by ENSO that have SILO counterparts, the coefficients of linear regression of seasonal-mean (top row) HiGEM SSTs on each HiGEM EOT, (second row) HadISST SSTs on each SILO EOT, (third row) HiGEM MSLP (contours) and 850 hPa winds (vectors) on each HiGEM EOT and (bottom row) 20th Century Reanalysis MSLP (contours) and 850 hPa winds (vectors) on each SILO EOT. Regressions of SST and MSLP are shown only where statistically significant at the 5 per cent level; wind vectors are drawn in black (gray) where significant (not significant) at the 5 per cent level.

## 6.2.2 Patterns driven by tropical cyclones

Two HiGEM EOTs, DJF EOT 4 (Fig. 11m) and MAM EOT 4 (Fig. 11n), are driven by variations in the number of tracks of tropical cyclones across northern and eastern Queensland. MAM EOT 4, however, is classified as an “extra” HiGEM EOT as it is the non-matching HiGEM EOT—no SILO MAM EOT is driven by tropical cyclones—that explains the least variance in the all-Queensland rainfall (Section 5.2), so it is analysed in Section 5.4. Only HiGEM DJF EOT 4, which matches SILO DJF EOT 2, is discussed further here.

As for SILO DJF EOT 2, HiGEM DJF EOT 4 shows no significant correlations with any of the large-scale drivers analysed here (Table 1). HiGEM DJF EOT 4 does, however, display significant correlations with tropical-cyclone track (Fig. 16a), genesis (Fig. 16b) and lysis (Fig. 16c) densities near the Cape York peninsula. The track and genesis densities suggest that this HiGEM EOT is associated with tropical cyclones that form in the Gulf of Carpentaria, then track southeast across the Cape York peninsula and out into the open ocean. This contrasts with SILO DJF EOT 2, in which cyclones form in the Coral Sea (Fig. 16e) before moving west across Cape York (Fig. 16d) and dying either there or in the Gulf of Carpentaria (Fig. 16f). Decreased 850–200 hPa vertical wind shear across northern and eastern Queensland accompanies high values of both HiGEM DJF EOT 4 (Fig. 16g) and SILO DJF EOT 2 (Fig. 16j); the spatial pattern of wind-shear anomalies is highly consistent between the model and 20CR.

Composites of tropical-cyclone tracks in the 40 seasons when HiGEM DJF EOT 4 is above (Fig. 16h) and below (Fig. 16i) one standard deviation show that seasons of high DJF EOT 4 are clearly associated with an increased number of tropical cyclones making landfall or approaching the Queensland coast. There are very few tracks near Queensland in low DJF EOT 4 seasons, despite having 40 seasons in the composite. The composites compare well with those from SILO DJF EOT 2, using IBTrACS data (Figs. 16k and 16l). Note that there are only six seasons each of the SILO composites, which leads to an obvious discrepancy with the HiGEM composites in the total number of tracks. Even though the tropical cyclones form to the west of Queensland in HiGEM, instead of to the east, HiGEM DJF EOT 4 corresponds well to SILO DJF EOT 2 in the region affected (northern Queensland), the mechanism (tropical cyclones) and the background conditions (reduced vertical wind shear).

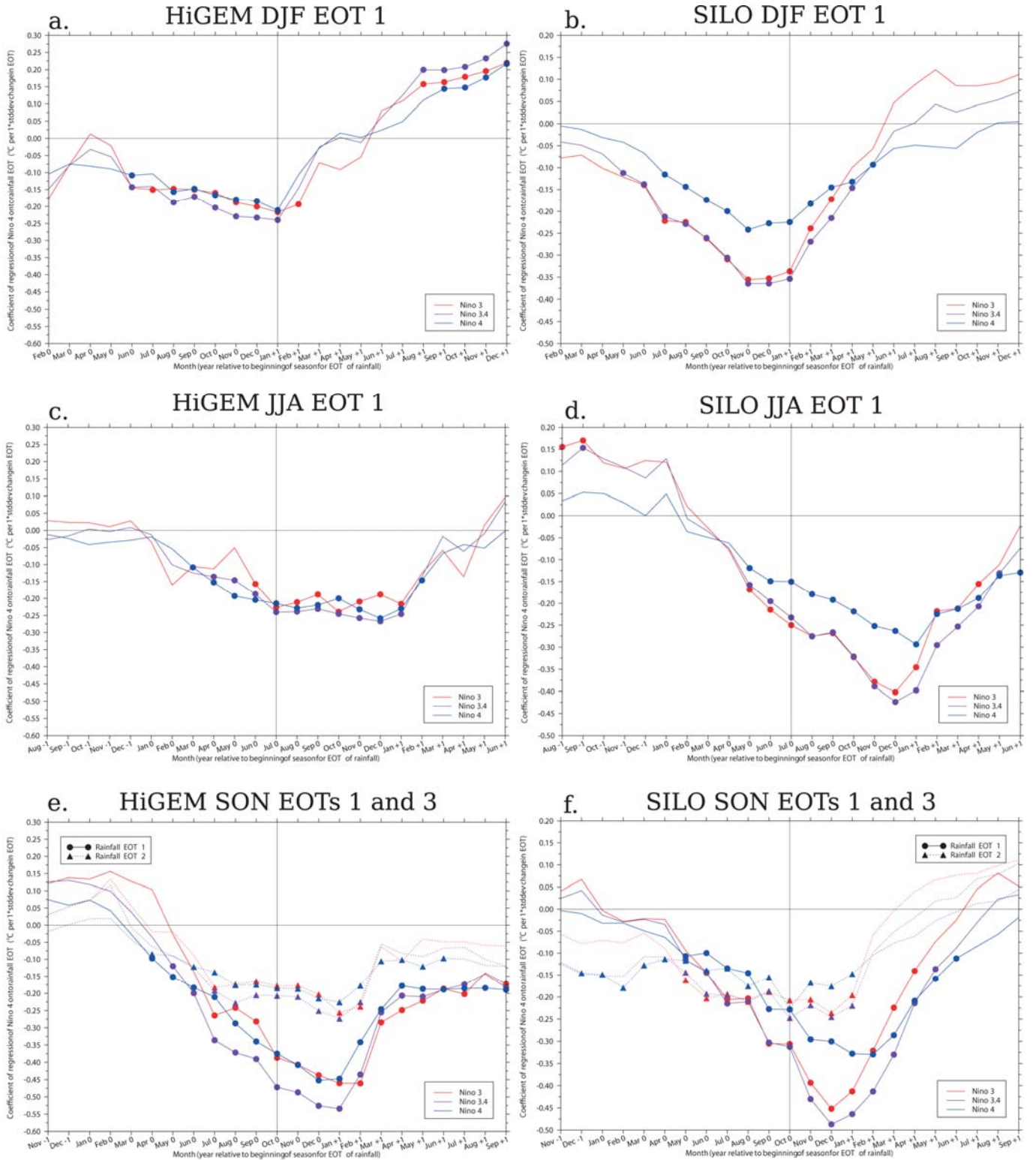


Figure 15: Lead-lag linear regressions of monthly-mean (red line) Niño 3, (purple line) Niño 3.4 and (blue line) Niño 4 SSTs on the time series of (left column) HiGEM EOTs and (right column) SILO EOTs. The solid vertical line gives the centre month of each three-month season. Symbols indicate where the regressions are statistically significant at the 5 per cent level.

### 6.2.3 Monsoon-driven patterns

HiGEM MAM EOT 1 is the only leading EOT that is not associated with ENSO (Table 1), consistent with SILO MAM EOT 1, which Klingaman (2012b) found was related to the strength of the late-season monsoon and local air–sea interactions. In HiGEM, MAM EOT 1 is linked to a weak enhancement of the monsoon cyclone, with stronger 850 hPa westerly winds and lower mean-sea-level pressures over northern Australia (Fig. 17a). These low-level circulation anomalies are far smaller than in SILO MAM EOT 1 (Fig. 17d), but show similar spatial patterns. HiGEM does not, however, reproduce the warm SST anomalies that were found in HadISST for SILO MAM EOT 1 (Fig. 17e), which supported the hypothesis that this EOT was driven by local air–sea interactions. Instead, HiGEM produces small areas of statistically significant warm anomalies that are almost certainly inconsequential (Fig. 17b). There are considerable increases in synoptic activity in HiGEM (Fig. 17f) - as measured by the standard deviation of MSLP2-10d, as in Klingaman (2012b) - across northern and eastern Australia, including Queensland, that resemble the increases found in 20CR (Fig. 17c). Thus, wet autumns in Queensland in HiGEM are associated with an increase in cyclonic systems crossing the late-season monsoon trough, but the monsoon circulation itself is not enhanced to nearly the same degree as in the corresponding SILO EOT.

The connection between HiGEM MAM EOT 1 and the late-season monsoon is reinforced by regressions of monthly rainfall for March–May onto the EOT time series (Figs. 17g–i). As for SILO MAM EOT 1 (Fig. 17j–l), HiGEM generates nearly all of the rainfall for this EOT in March, when the monsoon trough is typically retreating across northern Australia; the rainfall anomalies in April and May are negligible. Further, the pattern of March rainfall anomalies in HiGEM resembles that from SILO and is consistent with the mean position of the monsoon trough in March, which extends southeast from northern Western Australia through the Northern Territory and across Queensland to the border with New South Wales. Thus, state-wide Queensland rainfall variations in spring are driven by variations in the strength of the late-season monsoon in both observations and HiGEM, although the anomalous low-level cyclonic circulation is far weaker in the latter.

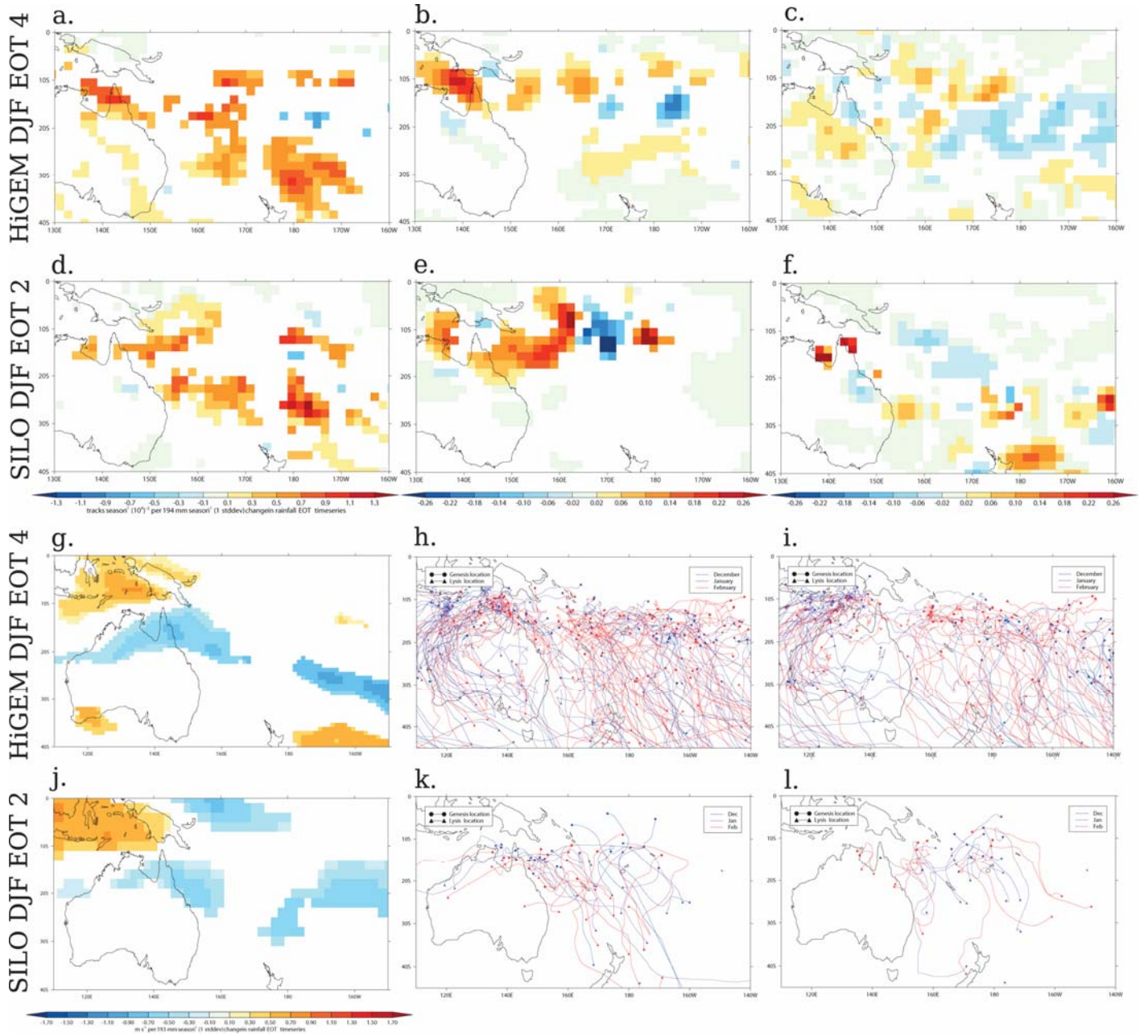


Figure 16: (a–c) Coefficients of linear regression of HiGEM (a) track, (b) genesis and (c) lysis densities (storms season<sup>-1</sup> 5° spherical cap at each grid point) on HiGEM DJF EOT 4; (d–f) as in (a–c) but for regressions of IBTrACS densities on SILO DJF EOT 2; (g) coefficient of linear regression of seasonal-mean HiGEM 850–200 hPa vertical wind shear on HiGEM DJF EOT 4; (h–i) composites of HiGEM tropical-cyclone tracks in seasons when DJF EOT 4 is (h) above and (i) below one standard deviation; (j–l) as in (g–i) but for 20CR vertical wind shear, IBTrACS tracks and SILO DJF EOT 2. Regression coefficients are shown only where statistically significant at the 5 per cent level.

## 6.2.4 Patterns driven by local circulations

Four of the SILO EOTs in Klingaman (2012b) were driven by variability in local synoptic patterns and circulations. Of these, three - DJF EOT 3 (Fig. 24c), MAM EOT 2 (Fig. 24f) and JJA EOT 2 (Fig. 24g) - were centred in southern and southeastern Queensland. All displayed decadal or multi-decadal variability, despite having no connection to any large-scale climate mode considered, leading Klingaman (2012b) to conclude that there was natural, independent decadal variability in the weather systems affecting Queensland.

Three of the four locally-driven SILO EOTs have HiGEM counterparts. The spatial pattern of HiGEM DJF EOT 2 (Fig. 11e) strongly resembles that of SILO DJF EOT 3. The 850 hPa circulation over Queensland is also similar to that from 20CR (compare Figs. 18a and 18d), with lower pressures off the east coast and an onshore flow into extreme southern Queensland. HiGEM produces much stronger MSLP and 850 hPa wind anomalies in the Southern Ocean than in 20CR, but the region of highest pressures southwest of New Zealand agrees well with 20CR. The mid-tropospheric (500 hPa) circulation and moisture anomalies are also consistent (compare Figs. 18b and 18e), with an anomalous cyclonic circulation over southeastern Australia and anomalously moist air along the southeastern Queensland coast and just offshore. Finally, there is increased variance in MSLP<sub>2–10d</sub> along the east coast in both HiGEM (Fig. 18c) and Fig. 18f). Despite overly strong Southern Ocean blocking, HiGEM DJF EOT 2 is clearly very closely related to SILO DJF EOT 3.

HiGEM MAM EOT 2 (Fig. 11f) is shifted east relative to SILO MAM EOT 2, which may be because HiGEM MAM EOT 1 (Fig. 11b) has considerable lower correlations in southeastern Queensland than SILO MAM EOT 1 (Fig. 24b). When the HiGEM MAM EOT 1 pattern was removed from the rainfall time series by linear regression, then, considerable more variance would have remained in southeastern Queensland, relative to the SILO rainfall time series after the removal of SILO MAM EOT 1, favouring southeastern Queensland for the HiGEM MAM EOT 2. The low-level circulation in HiGEM is also shifted, with anomalous cyclone off the east coast of Queensland (Fig. 18g) - similar to DJF EOT 2 - rather than over southeastern Australia as in 20CR (Fig. 18j). The mid-tropospheric pattern are remarkably similar, however (compare Figs. 18h and 18k) with convergence and anomalous high specific humidity along the Queensland coast. HiGEM also produces an increase in MSLP<sub>2–10d</sub> variance along the coast, which is slightly shifted east from 20CR, consistent with the shift in the rainfall maximum. Aside from the slight eastward movement of the centre of action in HiGEM, the two MAM EOT patterns are consistent: they affect southern and southeastern Queensland and are driven by anomalous cyclonic activity along the coast and onshore moisture transport.

Coherent variations in southeastern Queensland winter rainfall are described by JJA EOT 2 in HiGEM (Fig. 11g) and SILO (Fig. 24g). Anomalous 850 hPa onshore winds across southeastern Queensland are associated with both the modelled (Fig. 18m) and reanalysis (Fig. 18p) patterns, although HiGEM again exaggerates the spatial extent of the blocking in the Southern Ocean. This leads to positive correlations with blocking in both the 120°–150° E and 150° E–180° bands in HiGEM (Table 1), whereas the SILO JJA EOT 2 is correlated only with 20CR blocking in 150° E–180° only (Table 3). The HiGEM 500 hPa circulation (Fig. 18n) shows an anomalous anticyclone over central Australia that does not appear in 20CR (Fig. 18q), but HiGEM still produces onshore winds and weakly enhanced specific humidity near southeastern Queensland. The strong Southern Ocean blocking in HiGEM reduces MSLP<sub>2–10d</sub> variance across southeastern Australia (Fig. 18o), which is shifted south from 20CR (Fig. 18r). Still, the key driving mechanism for this mode—the increased blocking activity driving onshore winds—is well-represented in HiGEM.

In each of these three EOTs, HiGEM shows some decadal or multi-decadal variability (Figs. 13b–d). The variability does not persist throughout the integration, as it did throughout the observed record in Klingaman (2012b), but it is promising that HiGEM does produce some significant power on these timescales for these modes. This further strengthens the agreement between HiGEM and SILO in these EOTs.

One SILO EOT driven by local circulations does not have a HiGEM counterpart - JJA EOT 3 - and so is discussed in Section 4.3.2.

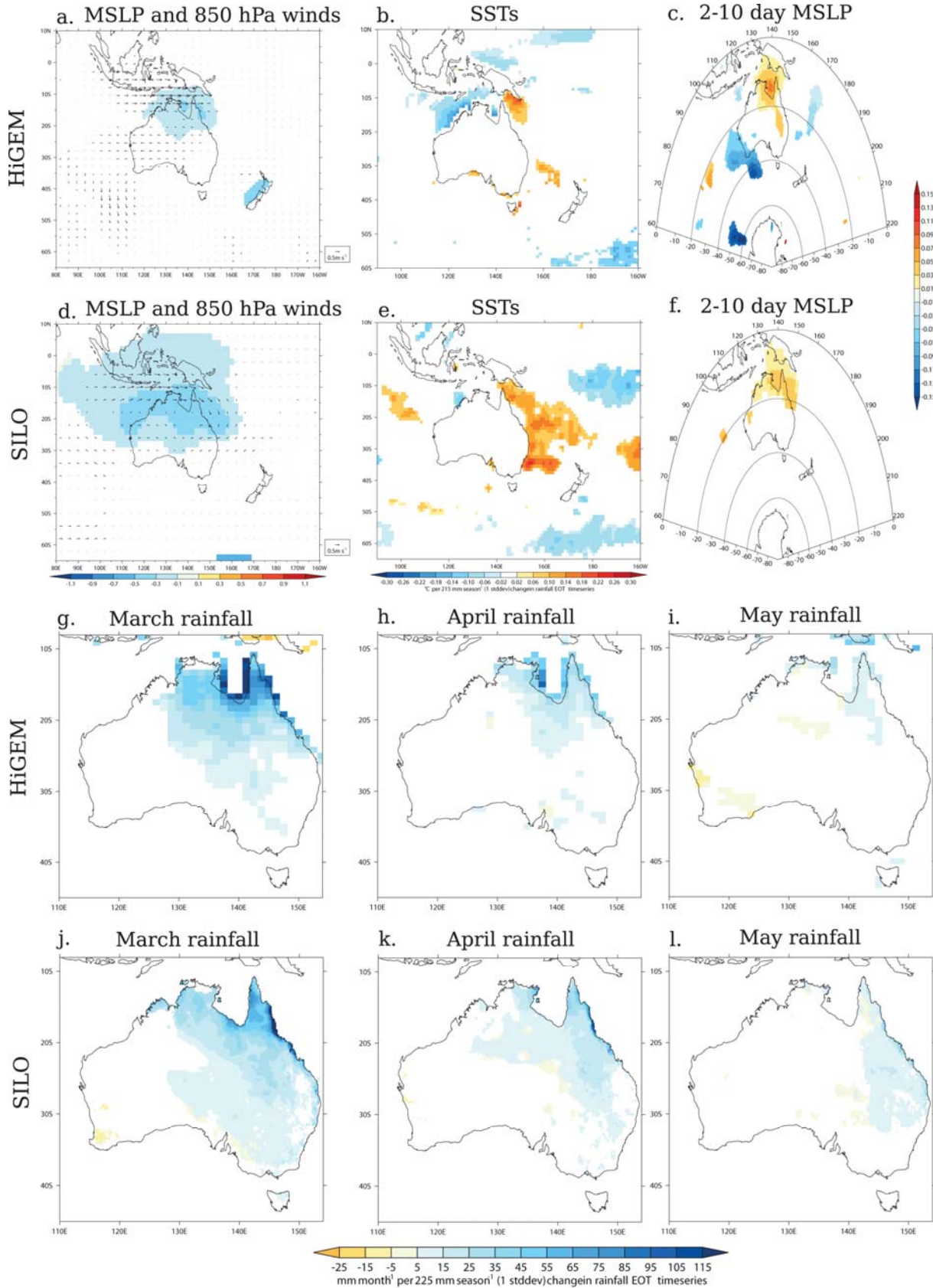


Figure 17: Coefficients of linear regression of (a–c) HiGEM (a) MSLP (contours) and 850 hPa winds (vectors), (b) SST and (c) standard deviation in MSLP<sub>2–10d</sub> on HiGEM MAM EOT 1; (d–f) as in (a–c) but using 20CR MSLP and HadISST SST on SILO MAMEOT 1; (g–i) HiGEM monthly rainfall for (g) March, (h) April and (i) May on HiGEM MAM EOT 1; (j–l) as in (g–i) but for SILO monthly rainfall on SILO MAM EOT 1.

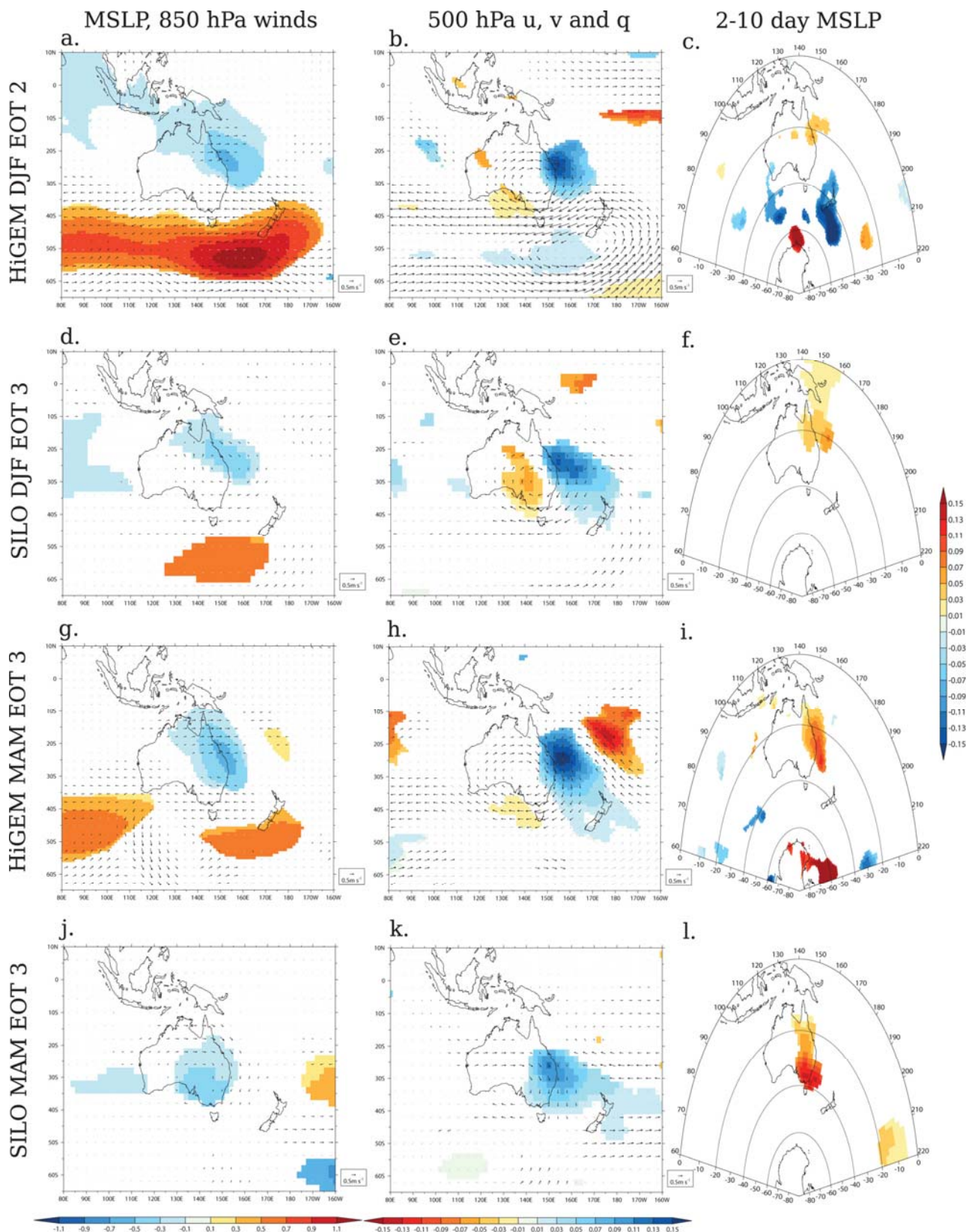


Figure 18: Coefficients of linear regression of (left) MSLP (contours) and 850 hPa winds (vectors); (centre) 500 hPa winds and specific humidity and (right) standard deviation in MSLP<sub>2-10d</sub> on (a-c) HiGEM DJF EOT 2, (d-f) SILO DJF EOT 3, (g-i) HiGEM MAM EOT 2, (j-l) SILO MAM EOT 2, (m-o) HiGEM JJA EOT 2, (p-r) SILO JJA EOT 2. HiGEM (SILO) EOTs use HiGEM (20CR) fields. Coefficients for MSLP and 500 hPa specific humidity are shown only where statistically significant at 5 per cent; wind vectors are drawn in black (grey) where significant (not significant) at 5 per cent.

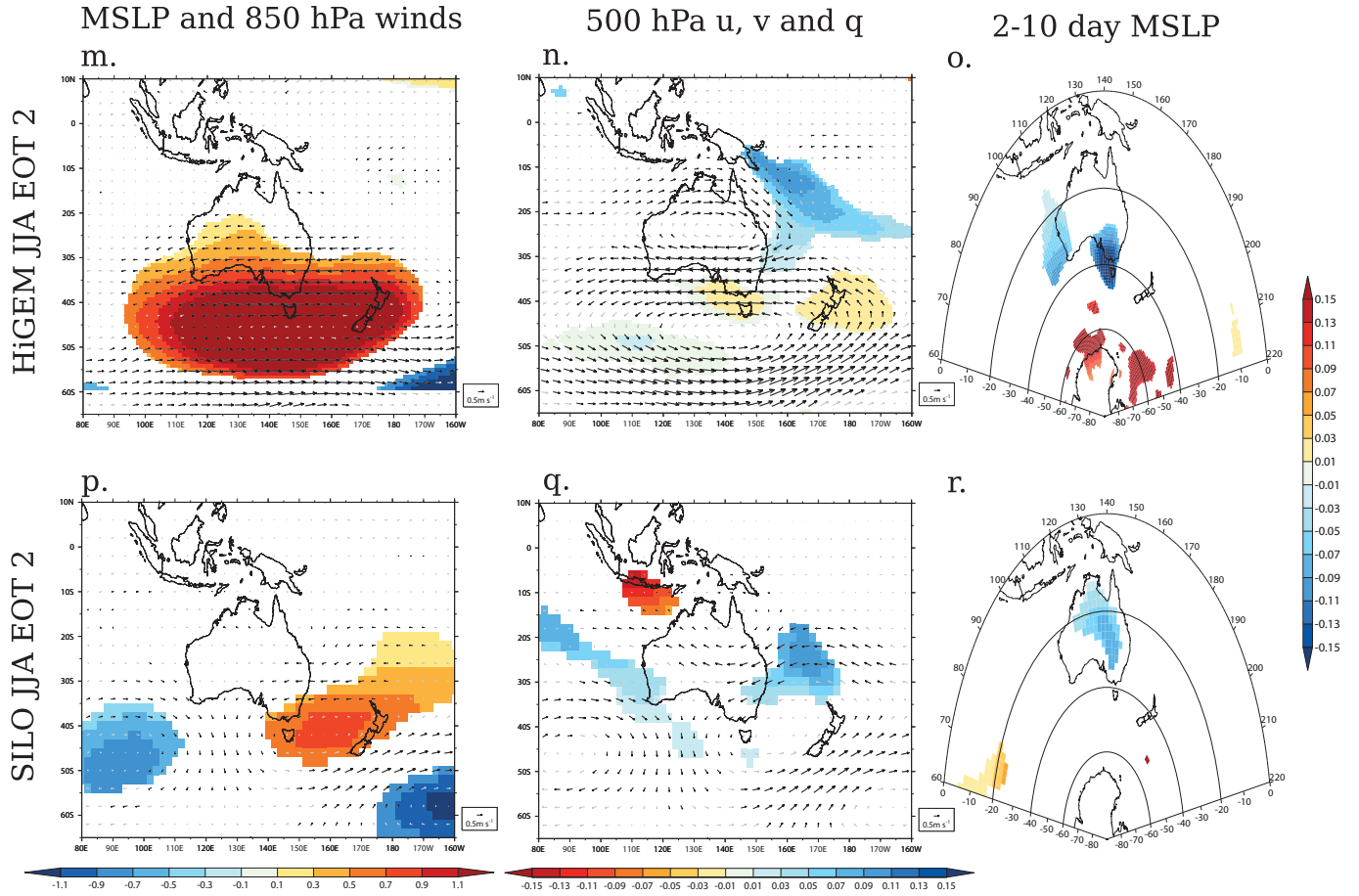


Figure 18 (continued)

### 6.2.5 SAM-driven patterns

Two HiGEM EOTs demonstrate statistically significant correlations with the SAM: SON EOT 1 and JJA EOT 2 (Table 1). Thus, HiGEM SON EOT 1 is correlated with both the SAM and ENSO (Section 5.2.1), as is its SILO counterpart (Table 3). Both EOTs also show significant partial correlations with the SAM when the influence of ENSO is removed from both the SAM and the EOT time series. MSLP anomalies associated with HiGEM SON EOT 1 show a clear annular signal (Fig. 19a) and are more pronounced than those from 20CR for SILO SON EOT 1 (Fig. 19b), particularly over Antarctica. It is important to note, however, that there are few surface-pressure observations in the Southern Ocean and Antarctica to constrain the 20CR, which may lead to errors in the 20CR in these regions and hence disagreement with the HiGEM MSLP regressions. The HiGEM and SILO EOTs are also positively correlated with blocking activity in the 120–150°E band; the 850 hPa wind regressions in HiGEM (Fig. 14i) show anomalous onshore winds across southern Queensland, consistent with strong anticyclonic activity in the Southern Ocean and the positive SAM phase.

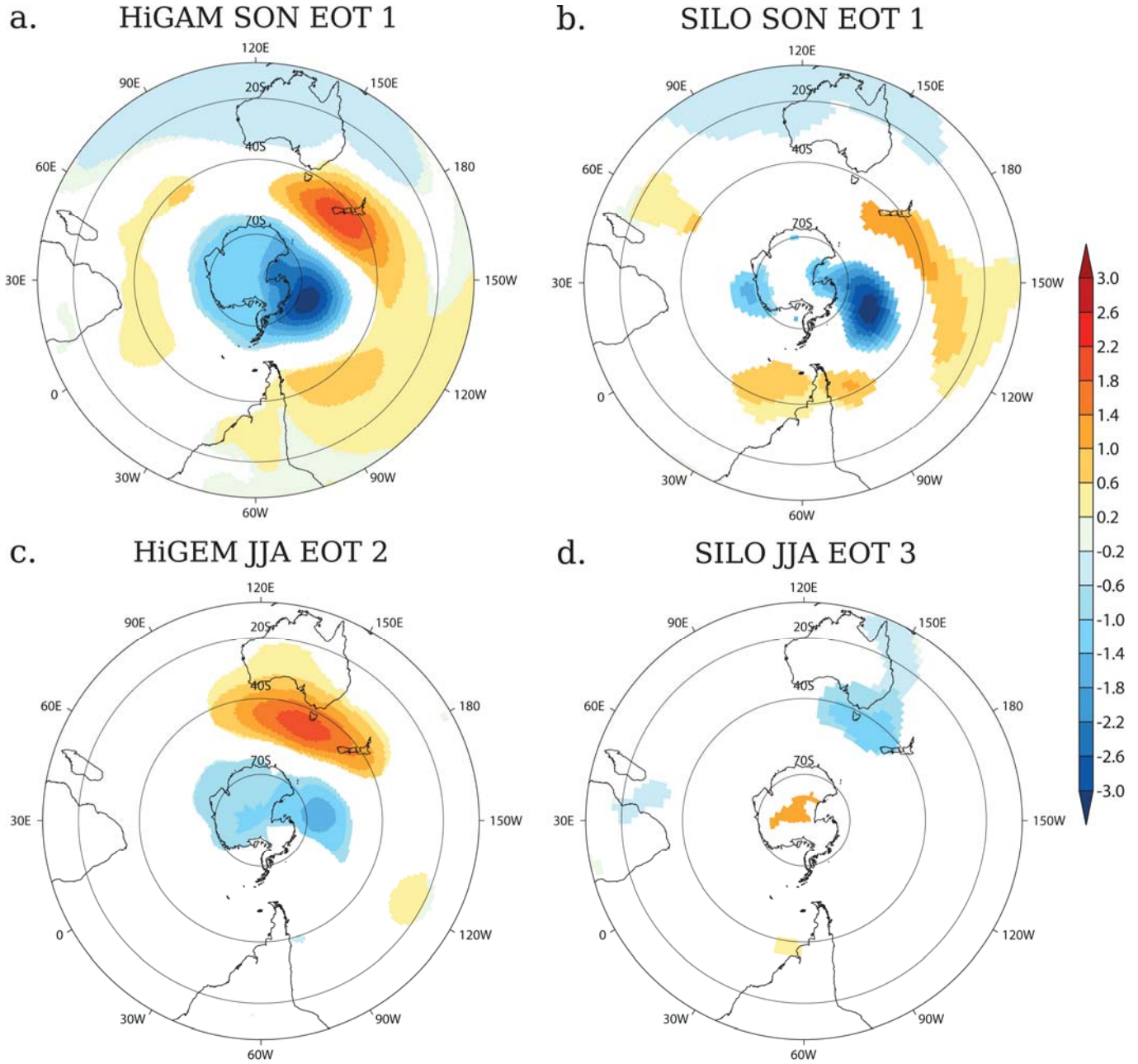


Figure 19: Coefficients of linear regression of (a) HiGEM MSLP on HiGEM SON EOT 1, (b) 20CR MSLP on SILO SON EOT 1, (c) HiGEM MSLP on HiGEM JJA EOT 2 and (d) 20CR MSLP on SILO JJA EOT 3. Regression coefficients are shown only where they are statistically significant at the 5 per cent level.

While HiGEM JJA EOT 2 shows a significant correlation with the SAM, but the MSLP regression pattern fails to show an annular structure at 40°S (Fig. 19c). This EOT was linked to blocking activity and onshore winds in Section 5.2.4; it is likely that the correlation with the SAM arises from the projection of the strong positive MSLP anomalies in the Southern Ocean south of Australia onto the positive SAM phase. Klingaman (2012b) identified similar behaviour, but of the opposite sign, for SILO JJA EOT 3, which showed a negative correlation with the SAM but only regional MSLP anomalies at 40°S (Fig. 19d). That EOT was linked to variability in coastal cyclones and the southward transport of tropical moisture (Table 4). The comparison between HiGEM JJA EOT 2 and SILO EOT 3 is made here not because they are driven by similar mechanisms, but because they demonstrate a statistically significant, but likely physically insignificant correlation with the SAM.

Like SON EOT 1, SILO JJA EOT 1 is correlated with both ENSO and the SAM (Table 3). HiGEM JJA EOT 1 is correlated only with ENSO. Its lack of a connection to the SAM will be considered in Section 5.3.3.

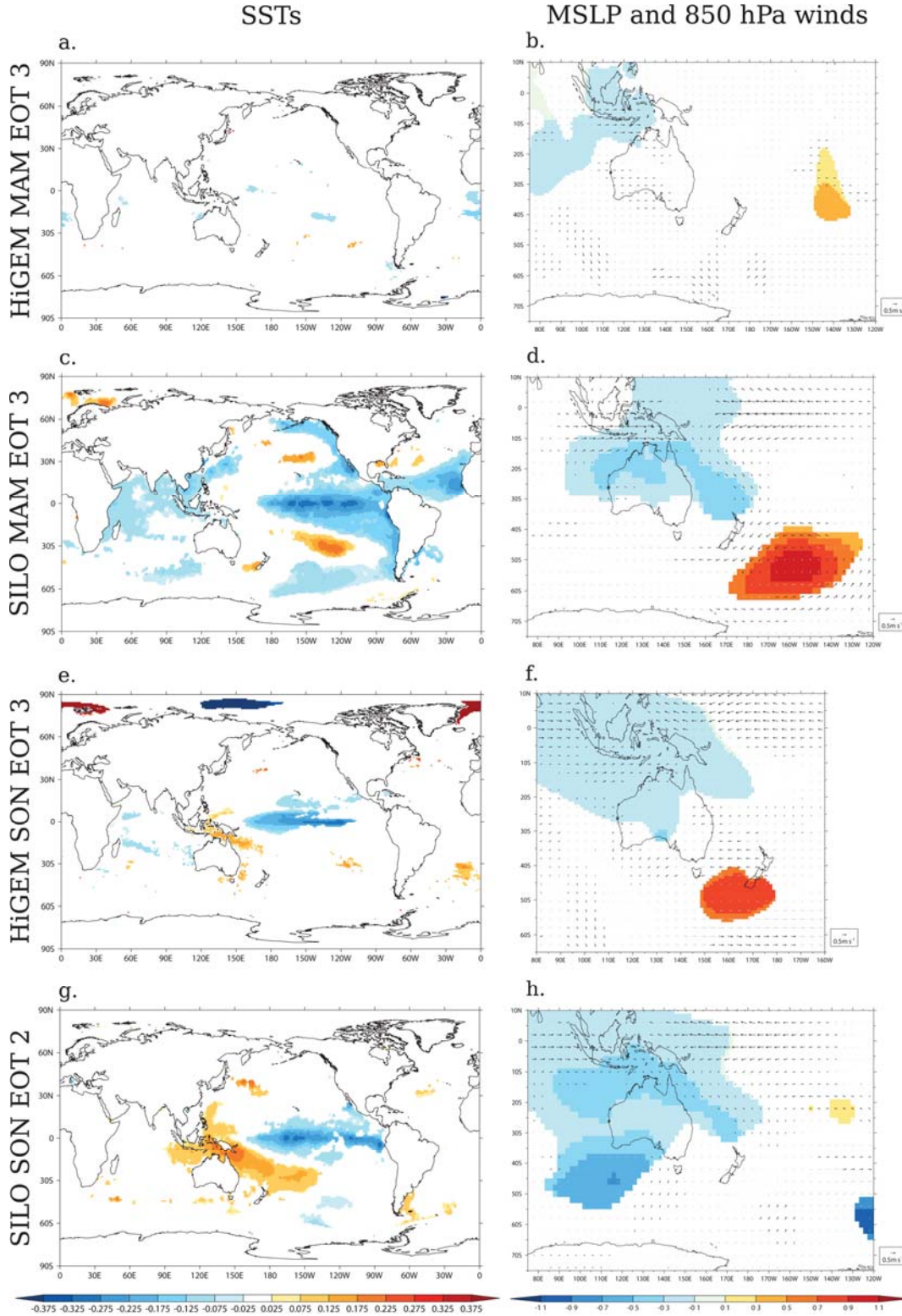


Figure 20: For (a, b) HiGEM MAM EOT 3, (c, d) SILO MAM EOT 3, (e, f) HiGEM SON EOT 3 and (g, h) SILO SON EOT 2, the coefficients of linear regression of (left column) SSTs and (right column) MSLP (contours) and 850 hPa winds (vectors) onto the EOT time series. Regressions for SILO EOTs use HadISST for SSTs and 20CR for MSLP and 850 hPa winds. For SST and MSLP, regressions are shown only where statistically significant at 5 per cent; 850 hPa winds are drawn with black (grey) vectors where statistically significant (not significant) at 5 per cent.